A Current Controller for a Switched Reluctance Motor
Based on Model Reference Adaptive Control

H.Naitoh and H. Ishikawa

Gifu University, 1-1, Yanagido, Gifu 501-1193, (*Japan*)

Abstract-- **Switched reluctance motors (SRMs) have some mechanically structural and electrical advantages. They also have disadvantages not only related to noise but also to nonlinearity in electromechanical responses. Unlike, for example, dc motors, the responses of current and torque of SRMs heavily depend on operating point associated with current and speed. Adaptive control based on model reference adaptive control is proposed for current control of SRMs. Experiment validates that the controller can regulate current response regardless of the operating points.**

Index Terms-- adaptive control, motor current, nonlinearity, switched reluctance motor

I. INTRODUCTION

In small motor applications, for example, in hybrid vehicles, magnetic motors have been widely used. One of the reasons is attributed to the magnet of neodymium-ferrite-boron (Ne-Fe-B). Although neodymium is a kind of rare metal, it is, in fact, not "rare". Its deposits are fairly abundant for rare metal. The magnet requires an additional component of dysprosium (Dy), which does not appear in the name of "Ne-Fe-B" but is indispensable to keep higher coercivity. Dy is also a kind of rare metal and really rare. The currently increasing demand for the Ne-Fe-B magnet will soon exhaust Dy in a couple of decades. The major users, for example, automobile manufacturers, cannot be optimistic about the promised future supply of the Ne-Fe-B magnet. Substitutional motors which are comparative to the Ne-Fe-B magnet motors and does not use magnet are, therefore, required.

Switched reluctance motors (SRMs) are robust, inexpensive, and easy to be manufactured owing to the absence of windings and permanent magnets in the rotors, which are simply made of iron and well suited for high-speed applications [1]. Other advantages include high peak torque-to-inertia ratios, fault-tolerant operation, and so forth [2].

Despite the above advantages, however, the following disadvantages are well known. They are high ripple content in torque, audible noise generation, electromagnetic interference noise generation, and so on [3]. From the viewpoint of current and speed control, the followings are substantial obstacles. Unlike dc motors,

and vector-controlled synchronous and induction motors, the generated torque of SRMs is not proportional to the armature current, but roughly proportional to the square of the current. This relationship is not consistent but varies depending on the operating points. Moreover, the transfer characteristic from input voltage to the input current is not known well. These drawbacks have prevented the widespread use of SRMs.

The drawbacks cause heavy nonlinearities in the controllability of SRMs. Ordinary linear controllers, for example, a proportional-integral controller cannot realize satisfactory responses of SRMs.

One way to overcome the above disadvantage is to dynamically adjust the control gains. The authors proposed an adjustable gain control strategy [4]. It employs integral control alone and an integral gain is tuned and tabulated in an off-line manner. Tabulation is, however, a quite time consuming task. Automatic adjustment in an on-line manner is quite preferable and desired.

This paper presents the application of model reference adaptive control (MRAC) to the current controller of an SRM. MRAC is a class of adaptive controls. Various adaptive control algorithms have been proposed [5] [6]. The MRAC employed in this paper is based on linear model following control (LMFC) and is the combination of an adaptive controller with LMFC [7] [8]. The adaptive capability of the controller is expected to compensate the nonlinearities of the SRMs.

In this paper, the drive configuration of SRM tested is overviewed first. The nonlinearity due to change in winding inductances and magnetic saturation is explained. The adaptive control algorithm is outlined. Experimental results are presented to validate the remarkable superiority of the MRAC-based controller over the nonlinearity of SRMs.

II. SRM DRIVE CONFIGURATION

The cross section of the 6/4 SRM used to test the proposed control is shown in Fig. 1; "6/4" indicates that the motor has six stator salient poles and four rotor salient poles. TABLE I lists the motor parameters. The drive circuit configuration is depicted in Fig. 2. The circuit is so called asymmetric H-bridge circuit. In this figure, three R+L branches equivalently represent the stator

windings of the motor. The SRM tested has three stator phases "A", "B", and "C". Each phase is composed of two windings around diametrically located stator poles. The rotor position θ is defined positive in the clockwise direction as shown in Fig.1. The $\theta=0°$ position corresponds to the phase "A" aligning with a stator pole.
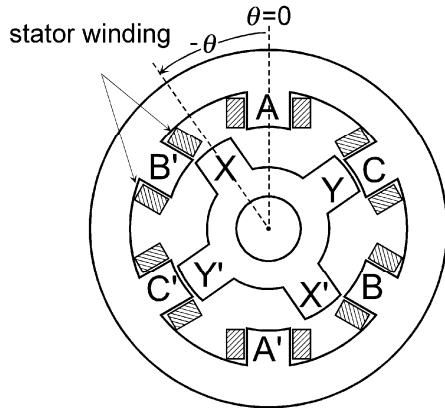
Fig. 1. 6/4 doubly salient SRM cross section.

TABLE I. PARAMETERS OF THE SRM TESTED

rated power	1.5kW
rated speed	1500 rpm
rated voltage	200 V
rated current	4.3 A
rated torque	9.55 Nm
stator phase number / pole number	3 / 6
rotor pole number	4

When the rotor is positioned as shown in Fig.1, for example, the switches S_{a1} and S_{a2} in Fig. 2 are on and the phase "A" is energized. The rotor pole tends to align with the energized phase in order to minimize the reluctance path. This is the motive forth to rotate SRMs. When the rotor pole X reaches the aligned position, the switches S_{b1} and S_{b2} are on instead of the S_{a1} and S_{a2} and so on. The SRM keeps rotating this way.
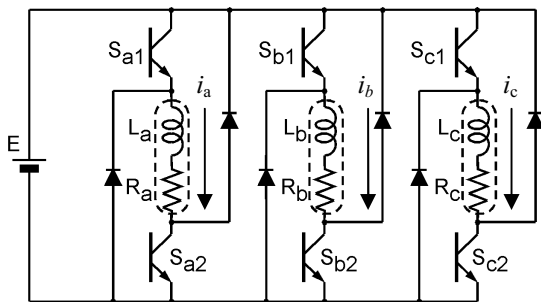
Fig. 2. Asymmetric H-bridge circuit.

In this paper, the energizing angle is fixed to $\theta= -35°$ at which two switches connected to a winding turn on simultaneously and the winding starts conducting. The upper switch takes PWM action to adjust the voltage supplied to the winding. At the angle of $\theta= -5°$, both switches turn off simultaneously. The carrier frequency of PWM is set to be 10kHz.

III. NONLINEARITY OF SRM

Figure 3 depicts the magnetic flux path at $\theta= -30°$ and $\theta= 0°$, respectively. The rotor rotates in the clockwise direction and the flux path changes with rotor position and with time. The stator winding inductance, therefore, varies with the change.
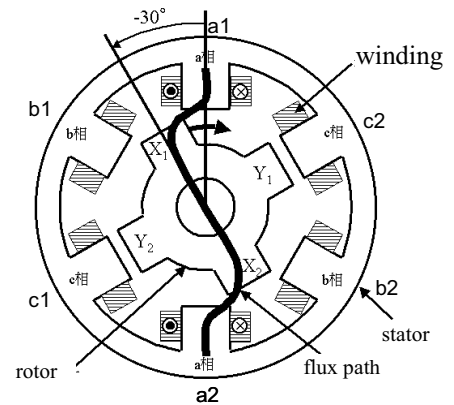
(a) rotor position $\theta=-30°$
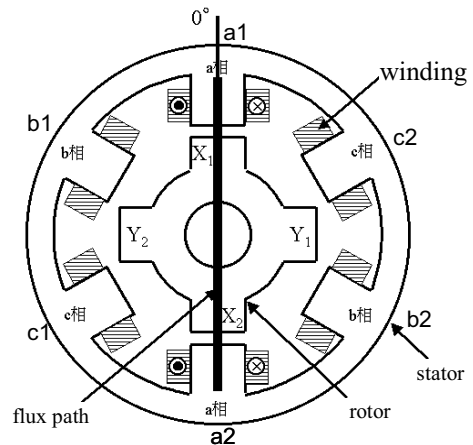
(b) rotor position $\theta=0°$

Fig. 3. Magnetic flux path.

Figure 4 shows variations of inductance $L(\theta)$ of the SRM tested with a phase current as a parameter; $L(\theta)$ is calculated using finite-element analysis and magnetic saturation is taken into account. In Fig.3, the plot for $i_a=0$ A is not affected by saturation. The $L(\theta)$ linearly increases for negative θ and decreases for positive θ. The plots for i_a larger than 0 A exhibits nonlinear plots due to saturation.

At the position in Fig. 3(a), torque is produced by the tendency of the salient-pole rotor to align with excited magnetic poles on the stator. Variation in $L(\theta)$ is, therefore, essential to produce torque for SRMs. SRMs must be designed such that the stator winding inductances vary. The electromagnetic torque of an SRM can be determined from the coenergy and given as

$$T_q = \frac{1}{2}\left(\frac{\partial L_a}{\partial \theta}i_a^2 + \frac{\partial L_b}{\partial \theta}i_b^2 + \frac{\partial L_c}{\partial \theta}i_c^2 \right) \qquad (1)$$
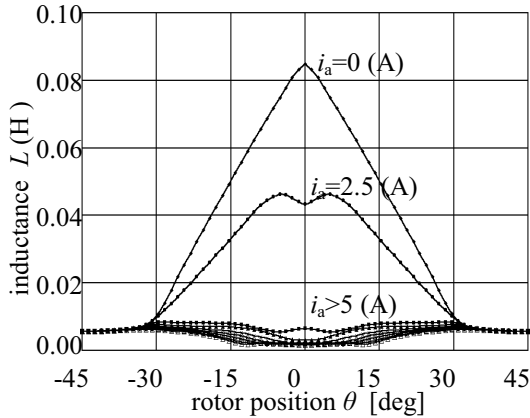
Fig. 4. Plots of inductance versus θ for the SRM tested.

where i_a, i_b and i_c are the phase currents[9][10]. The Eq.(1) indicates that the torque is proportional to the square of the phase currents. This torque formulation would be valid under the assumption that there is no rotor and stator-iron magnetic saturation. In practice, this assumption cannot be justified. The machine iron is usually driven significantly into saturation. Consequently, the relationship between the torque, inductances, and currents becomes more complex and is hardly formulated. The equivalent circuit of a phase winding is depicted as in Fig. 5, where E_B is back electromotive force.
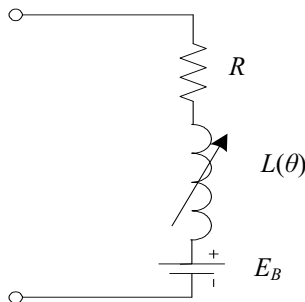
Fig. 5. Equivalent expression of a phase winding circuit elements

Ordinary linear controllers, for example, a proportional-integral (PI) controller with fixed gains is quite suitable for direct current motors and vector controlled induction and permanent magnet motors, for example, where the armature circuit elements are invariant and satisfactory responses can be achieved successfully. The PI controller is, however, almost useless for current control for SRMs, where, as mentioned above, the winding inductances are not constant.

Adaptive control which can sufficiently overcome the nonlinearity is vital to satisfactorily use of SRMs.

IV. MRAC ALGORITHM

Figure 6 shows a conceptual block diagram of model reference adaptive control system. The reference model and the controlled object are placed in parallel. The former specifies desired response characteristics. The

adjustable gains are placed in front of the object and dynamically adjusted in order to eliminate the difference between the outputs of the reference model and the controlled object. When the difference is driven to disappear, tracking of the output of controlled object to that of model is completed and the object behaves as desired.
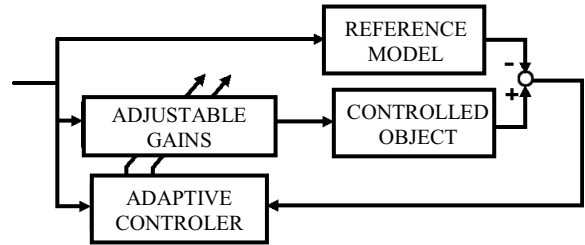
Fig. 6. Conceptual block diagram of model reference adaptive control system

The MRAC algorithm in this paper is as mentioned in ITRODUCTION based on linear model following control (LMFC) and can be referred to as AMFC (Adaptive Model Following Control) as well.

The block diagram of SRM current response is shown in time-discrete form in Fig.7 and the reference model in Fig. 8. Both the responses of actual SRM current response and the reference model are of the first order delay. The p, q, p_M, and q_M are defined as follows:
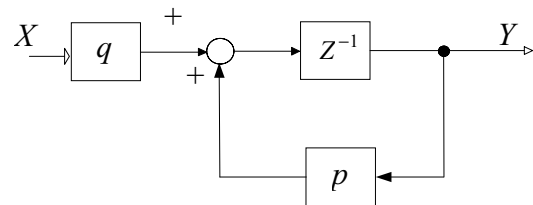
Fig. 7. Block diagram for SRM current response.
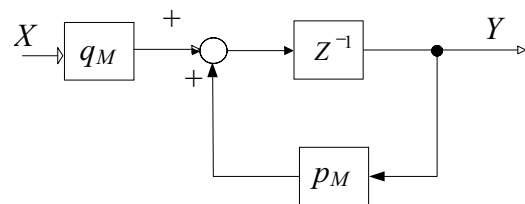
Fig.8. Block diagram of reference model

$$p = \exp(-T_C / T_S) \tag{2}$$
$$q = K (1 - p) \tag{3}$$
$$p_M = \exp(-T_{CM} / T_S) \tag{4}$$
$$q_M = K_M (1 - p_M) \tag{5}$$

where T_C and T_{CM} are the time-constants of the actual SRM current response and the model, respectively. The T_S is the sampling period.

Figure 9 presents the construction of a LMFC on which the MRAC algorithm is based. The objective of LMFC is
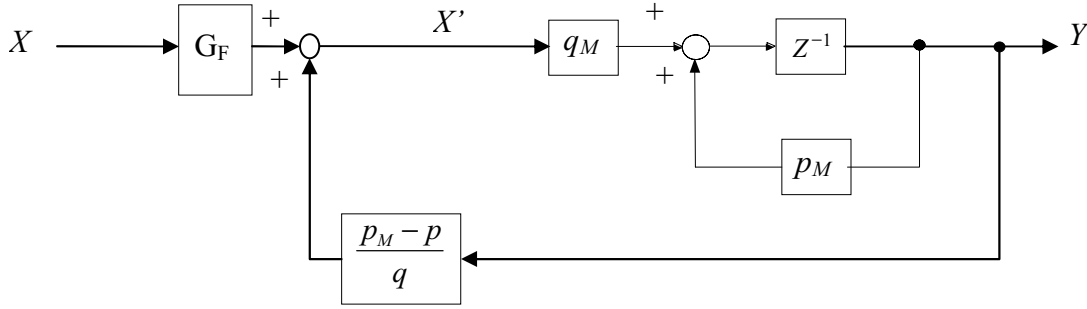
Fig. 9. LMFC based current controller configuration.
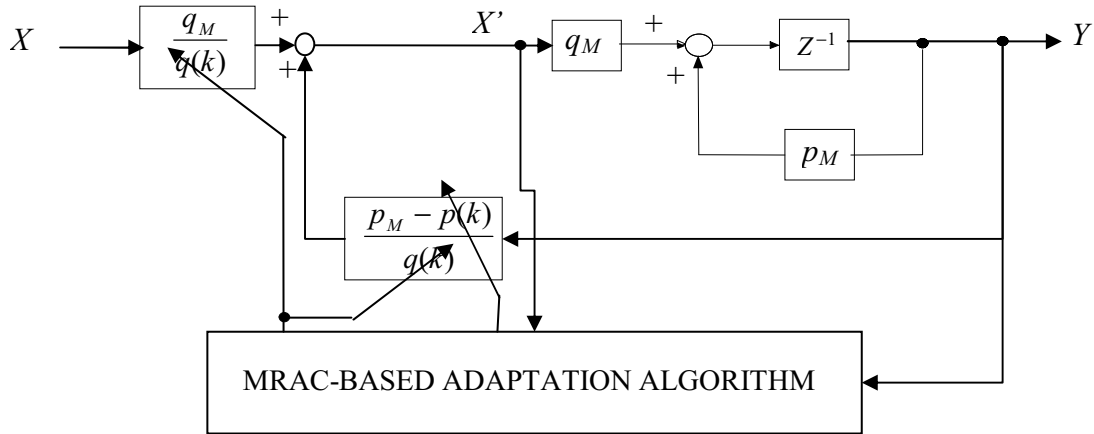
Fig. 10. Adaptive current controller configuration.

to make the response of SRM current follow that of the reference model. The compensation gains G_F and G_B placed in front of the controlled object as shown in Fig. 9 serve the above objective and in defined as follows.

$$G_F = \frac{q_M}{q} \qquad (6)$$

$$G_B = \frac{p_M - p}{q} \qquad (7)$$

A closer look at Fig. 9 indicates that it is identical to Fig. 8. The identity between them guarantees the model-following-capability of the LMFC.

The parameters p and q, in fact, vary during running due to change in the inductances of SRM. They are denoted by $p(k)$ and $q(k)$. Accordingly the compensation gains $G_F(k)$ and $G_B(k)$ can no longer be constant either. They should be adjusted during running through the estimation of $p(k)$ and $q(k)$:

$$G_F(k) = \frac{q_M}{q(k)} \qquad (8)$$

$$G_B(k) = \frac{p_M - p(k)}{q(k)} \qquad (9)$$

The adaptation mechanism takes care of the estimation as illustrated in Fig. 10. Note that unlike the conceptual block diagram in Fig. 6 no reference models are explicitly appear in Fig. 10. The correct and quick estimation of the $p(k)$ and $q(k)$ can reduce Fig. 10 to Fig. 9 and realize the current response to follow the adaptive model response.

The estimation algorithm is derived on the basis of the general theory of MRAC [7] and is summarized as:

$$p(k+1) = p(k) + K_P Y(k) E * (k+1) \qquad (10)$$

$$q(k+1) = q(k) + K_q X'(k) E * (k+1) \qquad (11)$$

where $E*(k)$ is the adaptive error and is defined as:

$$E*(k+1) = \frac{p_M E*(k) + Y(k) - [p(k)Y(k) + q(k)X'(k)]}{1 + K_P Y^2(k) + K_q X'^2(k)} \qquad (12)$$

The input reference $X'(k+1)$ to the SRM is then generated as:

$$X'(k+1) = \frac{[p_M - p(k+1)]Y(k) + q_M X(k)}{q(k+1)} \qquad (13)$$

V. EXPERIMENTAL RESULTS

A. Experimental setup

Experiment was performed on the 6/4 SRM outlined in Fig.1. The experimental setup is illustrated in Fig. 11. Three-phase ac is rectified by a diode bridge rectifier and
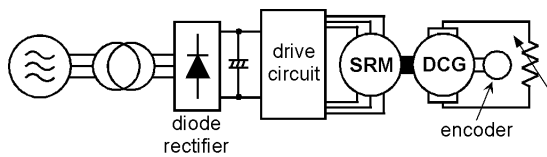
Fig. 11. Configuration of experimental setup

resultant dc is supplied to the drive circuit, that is, the asymmetric H-bridge circuit in Fig. 2. The switching devices are IGBT. The circuit regulates its output voltage in a PWM fashion with carrier frequency of 10 kHz. A dc generator with a variable resistor was coupled with the SRM and served as a load. A rotor position sensor is an incremental pulse encoder with resolution of $10000/360°$.

B. Current responses for conventional PI control

Fig. 12 shows simulation results for current responses with conventional PI control. The proportional and integral gains are tuned in such a way as to give a desired current step response of first-order delay with settling time of about 20msec at 1500 rpm. The current reference was changed stepwise from 2.0 A to 4.0 A. The result is shown in Fig. 12(a). The current wave form is that of periodical average over every commutation interval of 30° in mechanical angle equal to 60° in electric angle.

In Fig. 12(b) the motor speed is set down at 500 rpm with the same gains at 1500 rpm. The response in Fig. 12(b) exhibits violent oscillation. It can be concluded that the current can not be controlled at all. These simulation results clearly show the dependency of the current response on the motor speed. The response also depends on the magnitude of current although charts are not shown in this paper.

Because the peak value of current could exceed the rated current in experiment to damage the motor, the above discussion was done on simulation instead.

C. Current responses for MRAC

As shown in the previous section, the conventional PI control with fixed gains does not provide good current response over wide speed and current ranges.

Figure 13 presents experimental results of current responses. The current reference was changed stepwise from 2.5 A to 3.5 A. The control index, that is, the settling time is set to be equal to that for the conventional PI control. In Fig. 13(a), (b), and (c), speed is set at 1500 rpm, 1000 rpm, and 500rpm, respectively. These results demonstrate that, regardless of speed, the proposed MRAC-based controller can successfully regulate the motor current.

At 500rpm, the commutation period is 10 msec and comparable to the prescribed settling time. Actually two pulses are found in a span of 20 msec indicated in Fig. 12(b) and Fig. 13(c). Although the period is too coarse for control, the MRAC-based controller still keeps the desired control.
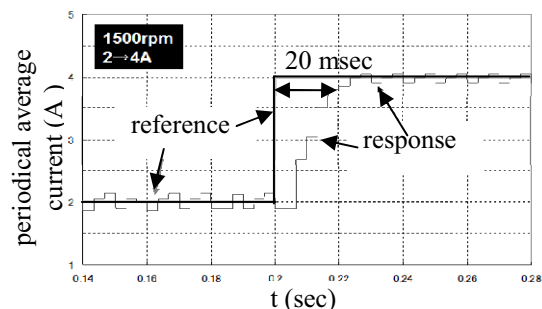
(a) current response at rotation speed: 1500rpm.
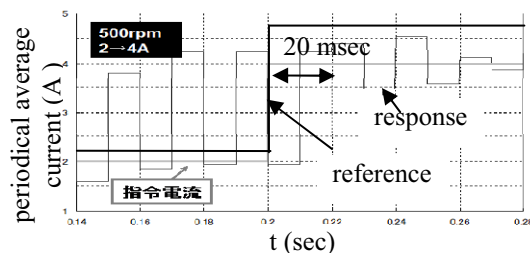
(b) current response at rotation speed of 500rpm.

Fig. 12. Simulation examples of stepwise current responses with conventional PI control.
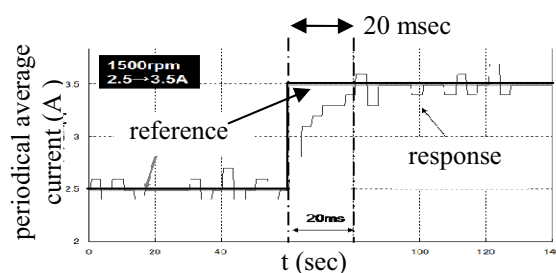
(a) current response at rotation speed of 1500rpm.
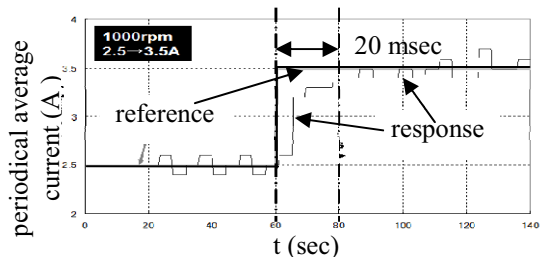
(b) current response at rotation speed of 1000rpm.
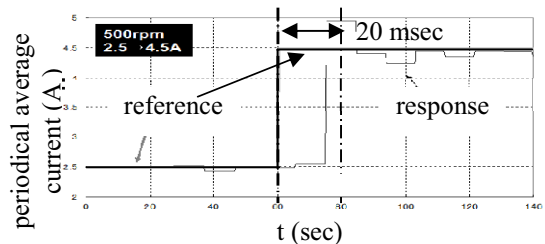
(c) current response at rotation speed of 500rpm.

Fig. 13. Experimental examples of stepwise current responses with MRAC.

VI. Conclusions

An adaptive control strategy based on MRAC was presented for current control of SRMs. The control algorithm and the configuration of the controller were established. Experimental results were presented to verify adaptation capability of the proposed MRAC-based controller in comparison with a conventional PI current controller.

Permanent magnet motors have been increasingly used for smaller capacity drive applications. Especially interior permanent magnet motors (IPMs) is preferred over the other type, that is, surface permanent magnet motors (SPMs). Torque of SPMs is so called magnetic torque which is ordinal one proportional to motor current like in dc motors and vector controlled induction and synchronous motors. That of IPMs consists of not only magnetic torque but also reluctance torque. Recent IPMs are so designed as to utilize more reluctance torque than earlier ones. IPMs employed by an automobile manufacturer for its hybrid vehicles, for example, generate more than half of total torque. The IPMs are no longer simply categorized into permanent magnet motor. They might be referred to as SRM with permanent magnet inserted. The nonlinear problem of reluctance torque is, therefore, vital to the motors as well. In order to surmount the problem the automobile manufacturer installs a quite complicated table in each hybrid vehicle to retrieve correct voltage reference to the inverter with keys of current, speed, and some other factors. The table is made in the factory before delivery. The task is very costly.

The MRAC-based control cannot directly control torque. A straightforward solution might be brought with direct detection of generated torque in an on-line manner. Torque sensors which can be installed in commercially products are not and maybe will not be available due to their detection principle where measurement of infinitesimally small torsion of a steel shaft is indispensable. A further challenge is to make the MRAC-based control applicable directly to torque control.

References

[1] N.Ertugrul, A.Cheok: *Indirect angle estimation in switched reluctance motor drives using fuzzy logic based motor model* , IEEE Trans. Power Electron. Vol. 15, No 5, Oct. 2000, pp. 1029-1044.

[2] V.Vujicic, N.Vukosavic : *A simple nonlinear model of the switched reluctance moto*r, IEEE Trans. Energy Convers., Vol. 15, No 4, 2000, pp. 395-400.

[3] Piyush, Tandon : *Self-tuning control of a switched reluctance motor drive with shaft position sensor*, Conf. Rec. of IEEE IAS Ann. meeting, 1996, pp.101-108.

[4] H. Ishikawa, H. Katoh, H. Naitoh: *Transfer Function Model for Linearized Torque Control for Switched Reluctance Motors*, Proc. of IPEC Niigata、April 2005, pp. 1660-1664.

[5] T. Cegrell, T. Hedqvist: Successful adaptive control of paper machines, Automatica, vol. 11, 1975, pp. 53-59

[6] C. G. Kallstrom, K. J. Astrom, N. E. Thorell, J. Eriksson, L. Sten: *Adaptive autopilots for tankers*, Automatica, vol. 15, 1979, pp. 241-254

[7] Y. D. Landau, *Adaptive Control.* : Marcel Deckker Inc., 1982, pp. 110-115

[8] H. Naitoh, S. Tadakuma: *Microprocessor-Based Adjustable Speed DC Motor Drives Using Model Reference Adaptive Control*, IEEE Trans. IAS, Vol. 15, No 4, April 1987, pp. 313-318.

[9] T. J. E. Miller: *Electric Control of Switched Reluctance Machines*, Newnes, 2001, pp. 54-61

[10] R. Krishnan: *Switched Reluctance Motor Drives*, CRC Press, 2001, pp. 49-11